

Article

# Characterization of Control-Dependent Variable Stiffness Behavior in Discrete Muscle-Like Actuators

Caleb Fuller <sup>†,\*</sup>  and Joshua Schultz <sup>†</sup> 

Department of Mechanical Engineering, University of Tulsa, Tulsa, OK 74104, USA; joshua-schultz@utulsa.edu

\* Correspondence: caleb-fuller@utulsa.edu; Tel.: +1-970-623-3859

† Current address: 800 S. Tucker Dr. Tulsa, OK 74104, USA.

Received: 5 February 2018; Accepted: 22 February 2018; Published: 28 February 2018

**Abstract:** This paper presents the modeling, characterization and validation for a discrete muscle-like actuator system composed of individual on–off motor units with complex dynamics inherent to the architecture. The dynamics include innate hardening behavior in the actuator with increased length. A series elastic actuator model is used as the plant model for an observer used in feedback control of the actuator. Simulations are performed showing the nonlinear nature of the changing stiffness as well as how this affects the dynamics, clearly observed in the phase portrait. Variable-stiffness hardening behavior is evaluated in experiment and shows good agreement with the model.

**Keywords:** actuators; variable stiffness; muscle-like actuators; discrete; control; Series Elastic Actuator (SEA) model

## 1. Introduction

Bio-inspired robotic actuator designs seek to emulate certain desirable traits seen in human skeletal muscle systems, and can sometimes exceed them in performance. The design presented in this article utilizes skeletal muscle characteristics, including: compliance, redundancy to failure, and a modular building block or cellular architecture, see Figure 1. One other concept taken from human skeletal muscle systems is that of motor unit recruitment [1]. Motor unit recruitment is a discretized actuation strategy that provides human skeletal muscle with a plan to generate the particular motion dictated by the nervous system. Each motor unit is responsible for recruiting certain muscle fibers, spread throughout the muscle, to achieve the contraction. In this way, if a contraction of higher strength is needed, more motor units are recruited. An actuation scheme based on this idea can simply change which motor units are activated if one motor unit suddenly is rendered broken or useless. Such an actuation device offers a high resistance to failure, which is a very attractive feature in high-reliability applications. The key advantage is that a component failure results not in a total loss of motion for that particular robotic limb, but only a decrease in performance, meaning a decrease in the maximum force that can be produced. A discrete actuator design that uses “on”–“off” motor units must utilize such a recruitment strategy for its actuation and control. There are challenges associated with quantizing an analog control signal into activating discrete units, which will be addressed by showing two methods of quantizing such a signal. The first method is a constant scaling of an approximation for the force, length and number of total motor units active. The second method is through the use of a pre-computed look-up table referenced during run time.

Compliance from unit-to-unit must also be a design component in order not to violate physical laws, as shown by Mathijssen et al. [2]. By introducing this compliance two things happen, the first is that it makes modeling the actuator very complex as each discrete unit now has an elastic element associated with it, but it also allows for the opportunity to vary the compliance in such a way as to introduce damping-like behavior where there was not before, which will be explained in more detail

later on. The units making up discrete actuators offer a redundancy that resists failure, for if one of the units is suddenly broken another unit can be recruited to “pick up the slack”. These three characteristics make discrete actuators very desirable for use in robotic applications of various types, but modeling the dynamics of these actuators becomes quite complex because each discrete unit must be treated as a mass-spring system, which results in very high order systems of differential equations. High order systems makes constructing a closed form control law difficult. This paper provides a method for overcoming these hurdles using a Series Elastic Actuator model and an observer system.

When modeling the dynamics of the actuator presented in this work, prior research in Series Elastic Actuators (SEAs) provides guidance in developing a controller to work with the actuator. An SEA was chosen to aid in the model development because its compliant element that operates in series with the motor is similar to the unit-to-unit compliance in a discrete muscle-like actuator. In the design of discrete actuators that are aligned in parallel formations there must be compliance coupling them together in order to adhere to physical laws. See Figure 2 for reference to this concept and read [2,3] for more detail.

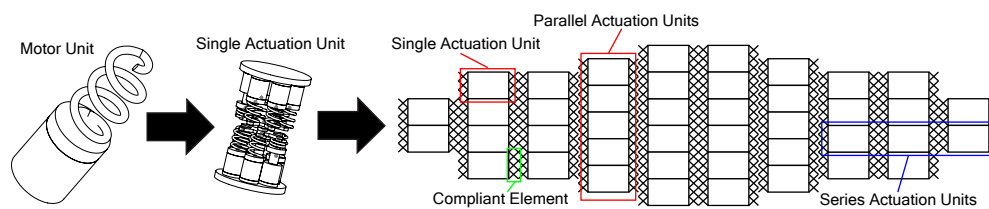


Figure 1. Modular, discrete muscle-like variable-stiffness actuator.

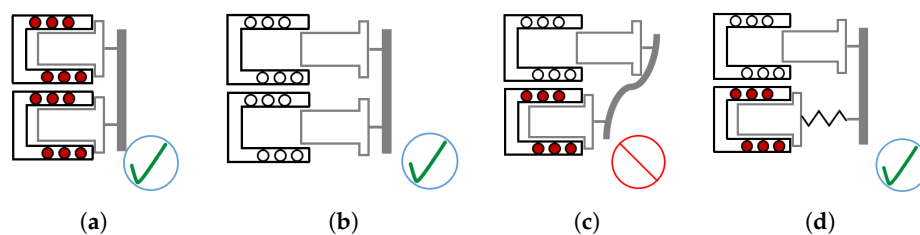


Figure 2. Compliance is necessary for allowing different contraction patterns for parallel motor units. See how in the third figure violation has occurred and is resolved by the addition of a compliant spring element in the fourth figure: (a) rigid connection for active units; (b) rigid connection for non-active units; (c) breaks laws of mechanics of materials; and (d) addition of compliant element.

The SEA was one of the earlier developments made in compliant actuators and provided a platform used as a basis for many of the later designs. Pratt and Williamson [4] developed an actuator that included a series elastic element that gives the actuator a compliant nature. More recent work in SEA’s has led to the development of Variable Stiffness Actuators (VSA), or Variable Impedance Actuators (VIA’s). Vanderborght et al. provide a definition for and discussion of the range of VSA’s and many of their characteristics in his overview of Variable Stiffness Actuators [5]. These actuators have numerous advantages (some of which have already been mentioned) including: compliance, the ability to reject disturbances due to the nature of their system dynamics, and the ability to be used in unpredictable environments. In his paper, Vanderborght also categorizes the different ways that variable stiffness is achieved in the many designs that have been developed. The three main categories are: active impedance control, inherent compliance and inherent damping, and inertial actuators. The actuator outlined in this work falls under the first and second categories. The actuator itself is defined by inherent variable stiffness and it can be actively controlled to vary this stiffness even more.

Discrete actuators have been implemented in the past with platforms seeking to control vibration and antenna shaping, see [6–10]. The main types of discrete actuators used in those applications

were piezoelectric, but the theoretical work done in this paper is able to be applied to many different types of discrete actuators. Discrete actuators are able to emulate human skeletal muscle with several distinctive characteristics. The first is *compliance*, which is a necessary characteristic in designing the actuator for applications where human–robot interaction is needed [11]. The second characteristic is *redundancy*, which is important because it achieves something that is novel and desirable for actuators, keeping the robot operational despite a component failure, which is an important characteristic when considering actuators that will be used in remote areas making repair difficult or impossible. The third characteristic is a *modular construction*; this is significant because the cost for expanding the actuator to new configurations or larger applications is low and the complex nature of redesigning an actuator for larger applications can be simplified if a framework for one of these actuators is already in place. This article seeks to provide such a framework for discrete actuators. A discussion on the actuator design will lead into showing the variable stiffness behavior seen most vividly in simulation, after which the capability of the SEA model will be shown, leading into a discussion on the control law developed through simulation, and finally an experiment with data showing the variable stiffness behavior.

## 2. Muscle-Like Actuators Composed of Discrete Building Blocks

Human skeletal muscle is made up of small discrete building blocks, which create the larger actuator. Coming from the perspective of control, our application begins with the motor units as the most fundamental. An actuation unit is the next step up from a motor unit, and is the reconfigurable unit for the actuator as a whole. A motor unit is defined as the “smallest individually activated force producing device”, while the actuation unit is defined as the “smallest building block of the actuator that can be inserted or removed” [2]. Putting these actuation units together into series and parallel bundles results in different arrays and arrangements providing the necessary configuration for the performance requirements of the task (Figure 1).

### 2.1. Actuation Unit Design and Definition

A discrete actuator is “a motion or force producing device composed of more than one actuation unit and containing more than one motor unit” [2]. The control paradigms presented in this article are based on the physical parameters of the platform built by Mathijssen et al., some details of which will be provided in Section 3. Other platforms will have many of the same features displayed in this design including: compliant spring element, modular actuation units, and mechanical stop/limiting component.

The motor units provide a small amount of displacement,  $\Delta x$ , extending the spring element thus producing a restoring force. To increase the force, one simply activates more motor units. See Figure 3 for an annotated graph depicting the various components of a discrete actuation unit.

Creating a usable lumped-parameter model of a compliant muscle-like discrete actuator that is able to be used in control development is not a simple problem. Schultz et al. [7] define a “class” structure to enumerate the types of different stiffness behaviors exhibited by the actuator at different lengths. However, this concept was only shown in simulation and the development of the idea did not explain what the actuator behavior is beyond the Critical Length. Thus, the work by Schultz et al. [7] did not provide a framework for the hardening behavior beyond this “Critical Length”.

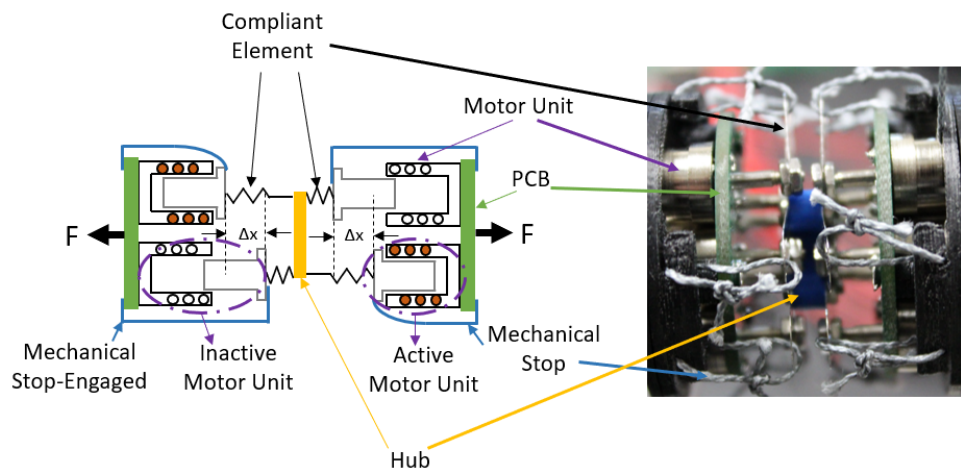


Figure 3. Actuation unit with annotated components.

### 2.2. The Mechanical Stop and Limiting Condition

To properly analyze and understand the hardening behavior of a discrete actuator one must understand how *mechanical stops* contribute to the system. The stops engage with the springs when an external force pulls on the units and extends them. In this actuator design the stops are attached to each lobe of the leaf spring. These stops give the actuator its variable impedance nature. When a load is placed across an actuation unit the spring begins pulling on the contraction mechanism. The springs on this actuator engage with the mechanical stops, shown in Figure 4, which prevent the inactive motor units from being dislodged and rendered useless. The mechanical stops keep the motor unit contraction mechanism (in this case, solenoid plungers) from pulling out of the motor unit housing (in this case, within the solenoid flux gap). However, when the springs encounter the mechanical stop the system dynamics of the actuator deviate from those of a typical spring-mass model. However, if the length of the actuator is stretched beyond this point then the spring deforms from the mechanical stops meaning the actuation units stiffness is a maximum stiffness of all the spring lobes in parallel. In this way before the particular spring lobe attached to the inactive motor units encounters the mechanical stop that spring element does not contribute to the overall stiffness of the actuator. That is the reason this actuator can vary the impedance through control of the different motor units.

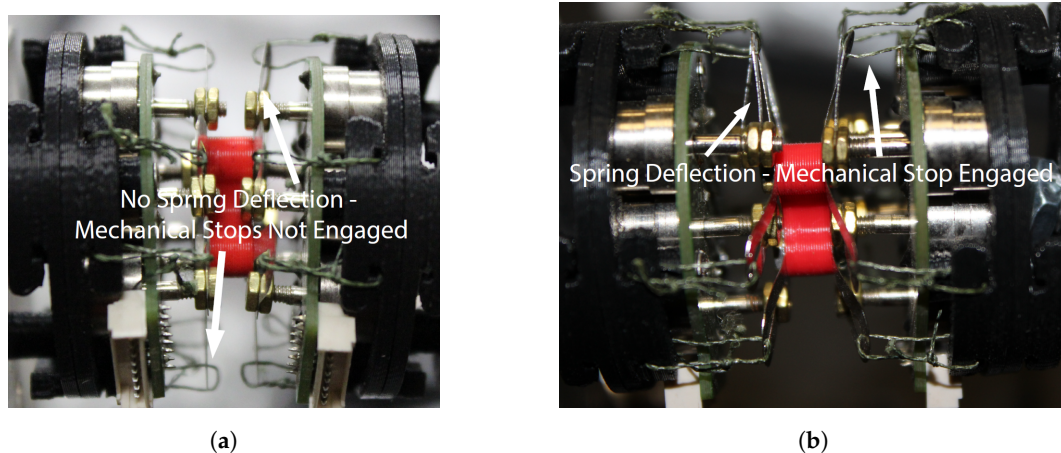


Figure 4. Demonstration of straps engaged with leaf-spring: (a) mechanical stop not engaged; and (b) mechanical stop engaged.

### 2.3. Class Structure

Four different classes of an actuation unit will now be defined. These class definitions help to understand how the dynamics of the actuator can be altered with changes of the various elements: motor units active, extension of the compliant element and the mechanical stop. After the definition and explanation of each Class, simulations showing the nonlinear variable stiffness qualities inherent in the design of the actuator will be shown, which exemplify how class affects the system dynamics. To begin a discussion of the class architecture describing the length-hardening behavior of the actuator, the resting length of the spring at two states must be defined, one when the actuation unit is active and the other when the actuation unit is inactive. At any given instant, an active actuation unit is a unit with *one or more* active motor units, while an inactive actuation unit is one with *no* active motor units. It is important to note that the actuation units move from one class to another during operation. It is assumed that there is at least some small pre-load  $\epsilon$  on the actuator at all time. The actuation unit can assume one of two distinct resting lengths. When an actuation unit has an active motor unit, whether it is one or  $n$  units active, the resting length is defined to be  $\ell^a$ . When an actuation unit has no active motor units, then the pre-load extends the actuation unit until the mechanical stops are encountered, which is defined as,  $\ell^o$ . The difference between the active resting length and the inactive resting length is the stroke length of the motor units,  $\ell_t = \ell^o - \ell^a$ . It is critical to note that the resting length for an actuation unit is the same regardless of whether one, two, three, or more motor units are active.

#### 2.3.1. Class 0

Class Zero is defined as being the state of the actuation unit when no motor units are active and the length of the actuation unit is less than the resting length,  $\ell^o$ , of the inactive actuation unit. This means the motor units are free to slide and move in and out of the metal casing of the motor units. For quasi-static motion (under the assumption of a small pre-load), Class Zero does not appear on any unit. Figure 5a shows the actuation cell in Class Zero.

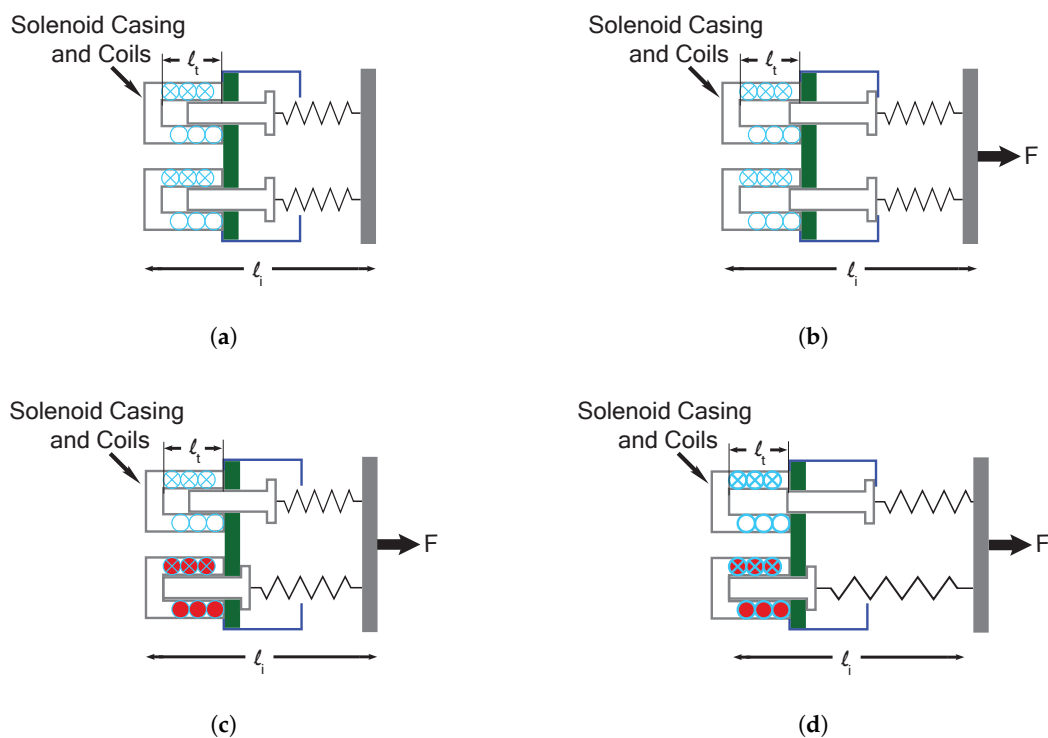


Figure 5. Variety in arrangements of actuators: (a) Class Zero; (b) Class I; (c) Class II; and (d) Class III.

### 2.3.2. Class I

Class I is defined as being the state of the actuation unit when no motor units are active and the length of the actuator has been extended beyond  $\ell^o$ . With an initial infinitesimal pre-load on the system this actuation unit will assume a resting length  $\ell^o$ , which is the length of the unit when resting against the mechanical stops. This can be seen in Figure 5b.

### 2.3.3. Class II

Class II is defined as being the state of the actuation unit when at least one motor unit is active and the length of the unit,  $\ell_i$ , is greater than the resting length of an active unit,  $\ell^a$ , but less than the length at which the mechanical stops are engaged,  $\ell^a < \ell_i < \ell^o$ . In this state the active motor units carry the load, while the inactive motor units are free to slide and move without carrying any load. In Class II, as the load approaches zero, the actuation unit will assume a resting length of  $\ell^a$ . Figure 5c shows a representation of an actuation unit in Class II.

### 2.3.4. Class III

Class III is defined for when the actuation unit has  $M$  active motor units, where  $0 < M < N$  ( $M = N \implies$  fully activated), and the unit has been stretched to a length that is beyond the mechanical stops,  $\ell^o$ . (For the platform presented in [2] the total number of motor units is  $N = 6$ ). Thus, for Class III both the active and inactive motor units are carrying the load for the actuator. However, this would manifest itself as a different stiffness than simply having 6 of the units in parallel because the compliant spring attached to the active motor units will be stretched an extra solenoid stroke length,  $\ell_t$ , further than the inactive motor units. Figure 5d shows a representation of an actuation unit in Class III.

### 2.3.5. Critical Length

Imagine that the actuator load quasi-statically stretches the actuator  $p$  units resting length to some length  $L$ . If the number of active motor units for each actuation unit  $i$  is given as  $p_i$ , then  $p_{min}$  is the minimum active over all  $i$  units. In [7], the term “Critical Length” is coined and is defined as the overall actuator length,  $L$ , when  $p_{min}$ , the weakest actuation unit (actuation unit with the fewest active motor units, and thereby the lowest stiffness), experiences extension and moves from Class II to Class III, where all the spring lobes of the inactive motor units engage with the mechanical stops and increase the overall spring constant of that actuation unit. It is important to realize that this will happen to each actuation unit individually at a different value of  $L$ , depending on how many motor units are active. One of the actuation units could be in Class III while another is in Class II and yet another could be in Class I. In extending the actuator’s length, the first actuation unit that will reach Class III is  $p_{min}$ . It should also be noted and is outlined in the three spring model from [7], that if there are more than one actuation units at  $p_{min}$  then these units will extend in length at the same rate and both move from Class II to Class III at the same value of  $L$ . Furthermore, given a total number of motor units active for the entire actuator, distributing them differently over the actuation units will result in a different Critical Length.

## 2.4. Activation Patterns and Activation Levels

There are many ways that the active and inactive motor units can be distributed over the actuation units that will total the same number of motor units active for the entire actuator, see Figure 6. The **activation level** is defined as the sum of active motor units on each actuation unit. Thus, if four actuation units are in series, two motor units could be activated on the first actuation unit, five motor units on the second, one motor unit on the third and zero on the fourth. This can be represented by the vector [2 5 1 0]. An example of a different **activation pattern** while keeping the same activation level would be [2 2 2 2]. However, another activation pattern that could be realized would be [6 2 0 0], each of these patterns totalling eight units active. However, specifying an activation pattern does not

determine *which* of the motor units on a given actuation unit are active, simply that two of the  $N = 6$  motor units are active. It should be evident that a large finite number of different stiffness values that depends on the number of actuation units and the number of motor units used to make up the actuator can be achieved. The following equations represent the activation level with  $M$  being the number of active motor units per actuation unit. In the example illustrated in this section, four actuation units  $P = 4$ , connected in series are used. Each actuation unit consists of one PCB with six motor units,  $N = 6$ , mounted on each PCB. The number of different stiffness levels that can be selected via the control input can be calculated using binomial coefficients and the equation for combinations seen in Equation (1).

$$\binom{n}{k} = \frac{n!}{k!(n - k)!} \tag{1}$$

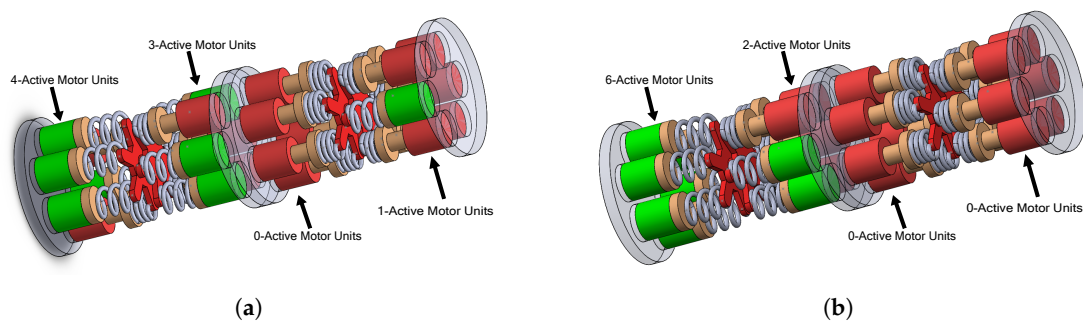


**Figure 6.** Different activation patters while maintaining same activation level: (a) eight motor units active (highlighted in green) over two actuation units—shorthand written as a vector [4 3 0 1]; and (b) eight motor units active (highlighted in green) over two actuation units—Shorthand written as a vector [6 2 0 0].

When calculating the number of stiffness levels ,substitutions for  $n$  and  $k$  can be made, as shown in Equation (2). In the substitution,  $N$  stands for the number of motor units used and  $P$  denotes the number of actuation units for the actuator following similar notation to [7]. This equation can be simplified to Equation (3).

$$\binom{N - 1 + P}{N - 1} = \frac{(N - 1 + P)!}{(N - 1)!((N - 1 + P) - (N - 1))!} \tag{2}$$

$$\frac{(N - 1 + P)!}{(N - 1)!(P)!} \tag{3}$$

For the length based hardening simulation that will be discussed later, if 0 is included as a state showing that there are no active motor units for that actuation cell, then four actuation units in series results in a total of 210 different stiffness levels that can be achieved through different activation patterns. For longer chains, it can easily be shown that by substituting the number of units in the equation for  $P$  and evaluating gives a determination for the new number of total activation levels.

As an individual actuation cell lengthens and moves from Class II into Class III, the overall stiffness of the actuator should increase. This is because the actuation cell moves from having less than the maximum number of motor units ( $M < N$ ) providing stiffness, to a point where the springs of the inactive motor units ( $N - M$ ) engage with the mechanical stops and begin providing stiffness to the overall spring constant. The exception is if all the motor units are active ( $M = N$ ) or all the motor units are inactive ( $M = 0$ ), in these cases there will not be a Class III distinction for this actuator or a critical length.

The stiffness of an actuator, made up of four actuation cells, increases in a nonlinear fashion as each of the cells moves from Class II into Class III. This happens in distinct steps because of the

difference in activation level between the four cells. The least active cell will reach Class III first, followed by the next least active cell and so on until the cell with the most active motor units reaches Class III. Once all the actuation cells have reached Class III and none are left in Class II the stiffness will remain constant with increasing length.

### 3. Complex System Dynamics of a Variable Impedance Discrete Actuator with a Simple SEA Observer Model

This section contains the simulations, results and discussion of driving an inertial load mass with an actuator made up of a chain of actuation units connected in series. Building upon the knowledge of the system variable stiffness behavior gained from the simulations, the equations of motion describing the actuator dynamics can be derived. These equations of motion include the hardening behavior presented in Section 2. This complex plant model is then simulated numerically under feedback control of the inertial load, with discretization of the control input, allowing us to observe the effects of the innate variable impedance behavior. However, before properly implementing the observer/controller, one needs to understand key ideas regarding a control system with discrete actuators.

1. A typical continuously variable signal  $u(t)$  will not be sufficient for driving a discrete actuator.
2. The control signal must be transformed into an integer number of motor units "on".
3. This number of motor units "on" must be selected based upon the closest value to the control signal that is possible.
4. One must decide which units will lead to the most desired affect on the system dynamics.
5. These steps are symplified by treating the entire actuator as an SEA.

In this section, there are three governing assumptions made about the system.

1. The contraction of the motor units is frictionless.
2. The mass of the actuation units is negligible as compared to the driven inertial mass.
3. The mechanical stops at each spring lobe engage at same length.

#### 3.1. Mathematica Formulation

Changing between the classes of the actuation units, which depends on the overall length of the actuator, is a nonlinear switching condition. The different classes of the actuator, discussed earlier in Section 2.3, give definition to the nonlinear phase portraits, a plot of the position versus velocity for the system, that will be shown and discussed in detail in this section. The setup in Figure 7 shows the simple actuator–mass–return spring configuration that was used in the simulations to be discussed shortly.

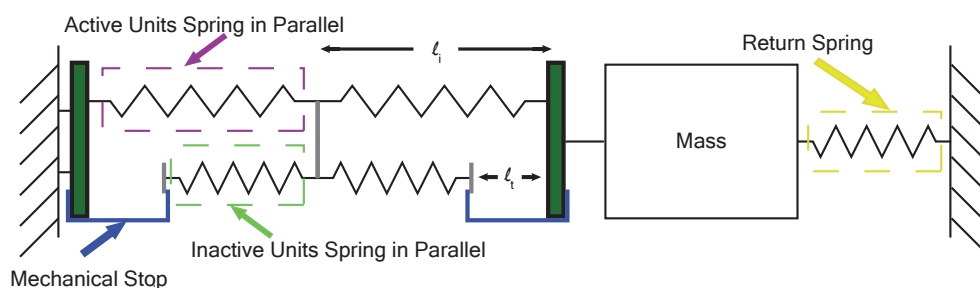


Figure 7. Horizontal oscillatory motion.

The equations describing the variable stiffness are not easily described in closed form due to the piecewise-linear behavior described in Section 2. Equation (4) gives the sum of the forces about the common node for two actuation units in a series chain connection,  $i$  and  $i + 1$ , as shown in Figure 7.

Table 1 displays the terms in the equation. The equation provides the force developed by a chain of actuation units based upon displacement and the stiffness, however this equation does not divulge which Class the actuation units are in, which is critical to knowing what the stiffness is for the actuator. The displacement of the actuation units,  $\ell_t$ , will be changing rapidly and the stiffness of the actuator will change according to which Class it is in, thus conditional statements must be used to check the Class of the actuator before computing force across the actuator.

$$\sum_i F_i : k_i^a (\ell_i - \ell_i^a) + k_i^{in} (\ell_i - \ell_i^o) = k_{i+1}^a (\ell_{i+1} - \ell_{i+1}^a) + k_{i+1}^{in} (\ell_{i+1} - \ell_{i+1}^o) \tag{4}$$

**Table 1.** Nomenclature for Equation (4).

Term	Description
$k_i^a$	spring constant active motor units in parallel
$k_{i+1}^a$	spring constant active motor units in parallel for next node in chain
$k_i^{in}$	spring constant inactive motor units in parallel
$k_{i+1}^{in}$	spring constant inactive motor units in parallel for next node in chain
$\ell_i$	length of actuation unit
$\ell_{i+1}$	length of next actuation unit in chain
$\ell_i^a$	resting length of active actuation unit
$\ell_{i+1}^a$	resting length of next active actuation unit in chain
$\ell_i^o$	resting length of inactive actuation unit
$\ell_{i+1}^o$	resting length of next inactive actuation unit in chain

In Equation (4), it should be noted that all  $\ell_i$  are unknown variables, and all  $\ell_i^a$  and  $\ell_i^o$  are known system constants. To properly identify the Class that each actuator resides in, the individual length of each actuator must be known. Therefore, the goal in arranging Equation (4) is to solve for those lengths,  $\ell_i$  and  $\ell_{i+1}$ . The total length of the chain of actuation units can easily be measured empirically by an encoder or similar sensor. In practice the  $\ell_i$  are not easily measured. A record of which motor units are active can also be obtained from the operating firmware. Therefore, the first step is to expand and collect the terms in Equation (4) about  $\ell_i$  and  $\ell_{i+1}$ . This gives the equation seen in Equation (5).

$$\ell_i (k_i^a + k_i^{in}) - \ell_{i+1} (k_{i+1}^a + k_{i+1}^{in}) = k_i^a \ell_i^a + k_i^{in} \ell_i^o - k_{i+1}^a \ell_{i+1}^a - k_{i+1}^{in} \ell_{i+1}^o \tag{5}$$

This will be simplified further by applying assumption (3), which says that all actuation units have the same active and inactive resting length,  $\ell_i^a = \ell_{i+1}^a = \ell^a$  and  $\ell_i^o = \ell_{i+1}^o = \ell^o$ , in practice there are slight manufacturing variations, but implementing this simplification results in Equation (6).

$$\ell_i (k_i^a + k_i^{in}) - \ell_{i+1} (k_{i+1}^a + k_{i+1}^{in}) = (k_i^a - k_{i+1}^a) \ell^a + (k_i^{in} - k_{i+1}^{in}) \ell^o \tag{6}$$

Dividing by  $k_i^a + k_i^{in}$  gives Equation (7). Then, a change of variable can be made setting  $a_i = \frac{(k_{i+1}^a + k_{i+1}^{in})}{(k_i^a + k_i^{in})}$ , which gives Equation (8).

$$\ell_i - \ell_{i+1} \frac{(k_{i+1}^a + k_{i+1}^{in})}{(k_i^a + k_i^{in})} = \frac{(k_i^a - k_{i+1}^a)}{(k_i^a + k_i^{in})} \ell^a + \frac{(k_i^{in} - k_{i+1}^{in})}{(k_i^a + k_i^{in})} \ell^o \tag{7}$$

$$\ell_i - \ell_{i+1} a_i = \frac{(k_i^a - k_{i+1}^a)}{(k_i^a + k_i^{in})} \ell^a + \frac{(k_i^{in} - k_{i+1}^{in})}{(k_i^a + k_i^{in})} \ell^o \implies \begin{cases} \text{Class 0,} & \text{undefined} \\ \text{Class I,} & k_i^a = 0 \\ \text{Class II,} & k_i^{in} = 0 \\ \text{Class III,} & k_i^a \neq 0 \ \& \ k_i^{in} \neq 0 \end{cases} \tag{8}$$

Notice the conditional statement introduced that allows this general equation to be used for Class Zero–Class III (definitions of which can be found in Section 2.3). Equation (8) represents the force–length relationship for actuation units in Class III. However, in order to adjust this to be used with a unit in Class II the term  $k_i^{in}$  must be set equal to 0. This is the term quantifying the spring constant once the units have reached critical length and extend beyond the mechanical stops. Setting this equal to zero and substituting into Equation (8) will give a correct representation of the sum of forces for this Class.  $a_i$  will change to:  $a_i = \frac{(k_{i+1}^a + k_{i+1}^{in})}{k_i^a}$ . If, however, the unit is in Class I, then the motor units on board the actuation unit are all contributing to the stiffness and are all inactive and the length has been extended beyond the inactive resting length,  $\ell_i > \ell^0$ . If this is the case, then substituting  $k_i^a = 0$  into the equation for  $a_i$  and Equation (8) will correctly categorize the sum of the forces for this state of the actuator. The last Class is Class Zero for which the force across the actuator is zero and neither the inactive nor the active motor units contribute to carrying the load. In this case, the load is only across the return spring seen in Figure 7, which corresponds to Equation (7) being undefined for Class Zero.

These equations and conditions can then be written for any number of actuators in series and put in matrix form as seen in Equations (9)–(12). Whereas the  $a_i$  matrix is defined in Equation (10),  $c_i$  is defined in Equation (12), and the individual actuation unit lengths are given by Equation (11).

$$A \cdot \ell = C \tag{9}$$

$$A = \begin{pmatrix} 1 & -\frac{k_{i+1}^a + k_{i+1}^{in}}{k_i^a + k_i^{in}} & 0 & \cdots & 0 \\ 0 & 1 & -\frac{k_{i+2}^a + k_{i+2}^{in}}{k_{i+1}^a + k_{i+1}^{in}} & \ddots & \vdots \\ \vdots & \ddots & \ddots & \ddots & 0 \\ 0 & \cdots & 0 & 1 & -\frac{k_n^a + k_n^{in}}{k_{n-1}^a + k_{n-1}^{in}} \end{pmatrix} \tag{10}$$

$$\ell = \begin{pmatrix} \ell_i \\ \ell_{i+1} \\ \vdots \\ \ell_n \end{pmatrix} \tag{11}$$

$$C = \begin{pmatrix} \frac{k_i^a - k_{i+1}^a}{k_i^a + k_i^{in}} \cdot \ell^a + \frac{k_i^{in} - k_{i+1}^{in}}{k_i^a + k_i^{in}} \cdot \ell^0 \\ \frac{k_{i+1}^a - k_{i+2}^a}{k_{i+1}^a + k_{i+1}^{in}} \cdot \ell^a + \frac{k_{i+1}^{in} - k_{i+2}^{in}}{k_{i+1}^a + k_{i+1}^{in}} \cdot \ell^0 \\ \vdots \\ \frac{k_{n-1}^a - k_n^a}{k_{n-1}^a + k_{n-1}^{in}} \cdot \ell^a + \frac{k_{n-1}^{in} - k_n^{in}}{k_{n-1}^a + k_{n-1}^{in}} \cdot \ell^0 \end{pmatrix} \tag{12}$$

Looking at these equations, one can see that deliberately picking which motor units are activated alters the distribution of active motor units across the actuation units, allowing a tunable hardening behavior for the system dynamics, or an introduction of damping-like behavior without any damping in the system (see Corr and Clark [8]). This is demonstrated in the following section as the phase portraits are examined, which is a common tool for analyzing nonlinear dynamic systems.

### 3.2. Simulations and Illustrative Examples of Discrete Muscle-Like Actuator Dynamics

The best way to present the information described in the previous section is to contrast a single-ended actuator with a return spring in an antagonist setup, as shown in Figure 7. Pure simple harmonic motion for such an antagonist setup would give a uniform ellipsoid.

Using the matrix definitions in Equations (10)–(12), the equations of motion can be simulated to analyze the oscillatory motion of a mass attached to the end of a muscle-like actuator as seen in the

setup of Figure 7. In these simulations, a setup of two actuation units was chosen each with six motor units. Choosing two actuation units allows the actuator to display the discretization effects seen in the phase portraits and control input, however, the theoretical formulation developed in the previous section is valid for  $n$  units in a chain and for any number of motor units per actuation unit, and it can also extend easily to bundles of chains. Adding more actuation units decreases the discretization effects making it appear more and more linear until at some point the quantization is so linear it can be more or less considered continuously variable. However, most practical applications will have a small enough number that quantization is necessary. There are four cases shown in Figure 8: (1) a simple harmonic motion between a linear spring and our actuator; (2) a switching method based on time; (3) a switching method based upon actuator position, right or left of the origin; and (4) a switching method based on the sign of the velocity, so above or below the origin. Thus, it can be said that the third and fourth methods are a type of quadrant based switching, but with a limited number of activation patterns and activation levels dictated by the number of actuation units and their arrangement within the actuator. In all of these figures, activation level is held constant but the activation pattern is varied.

1. Figure 8a shows the phase portrait of the natural response of the muscle-like actuator due to an initial condition (blue), contrasting a linear spring setup showing the familiar symmetrical ellipse pattern. The “D” shape curve clearly shows the hardening behavior. The three vertical lines show the points at which the actuation units move from Class II to Class III, the first vertical line closest to the origin being the Critical Length of the actuator.
2. Figure 8b looks at the phase portrait in which the actuator switches between two different activation patterns halfway through the simulation time. It is evident the phase portrait changes shape, and is easy to tell that the second pattern has a higher stiffness than the first.
3. Figure 8c displays a switching pattern that changes the activation pattern at equilibrium position. It is evident that this switching pattern does not offer the stark difference between activation patterns, and thus it should be noted that as long as the actuator is in Class Zero it has no hardening behavior, this also means that as long as the oscillation has a negative position on the phase portrait it is only affected by the return spring and carries none of the aspects of the variable stiffness muscle-like actuator.
4. Figure 8d shows a switching condition based upon the velocity of the load mass, which can easily be measured in practice. Velocity switching occurs by moving from an actuation pattern that is less “stiff” to an actuation pattern that is more “stiff” at the point when the velocity sign changes; it can be noted that this can be done with the same total number of motor units active across the actuation units (but changing the distribution) or by increasing the number of total active motor units. The results from this simulation, see Figure 8d, are quite interesting. For the mass fixed to the end of this actuator and a return spring it exhibits damping-like behavior without there being any damping modeled in the system.

Switching control is a method of control used in practice and has been shown by Gasparri et al. to be a feasible control scheme for his variable stiffness actuator [9].

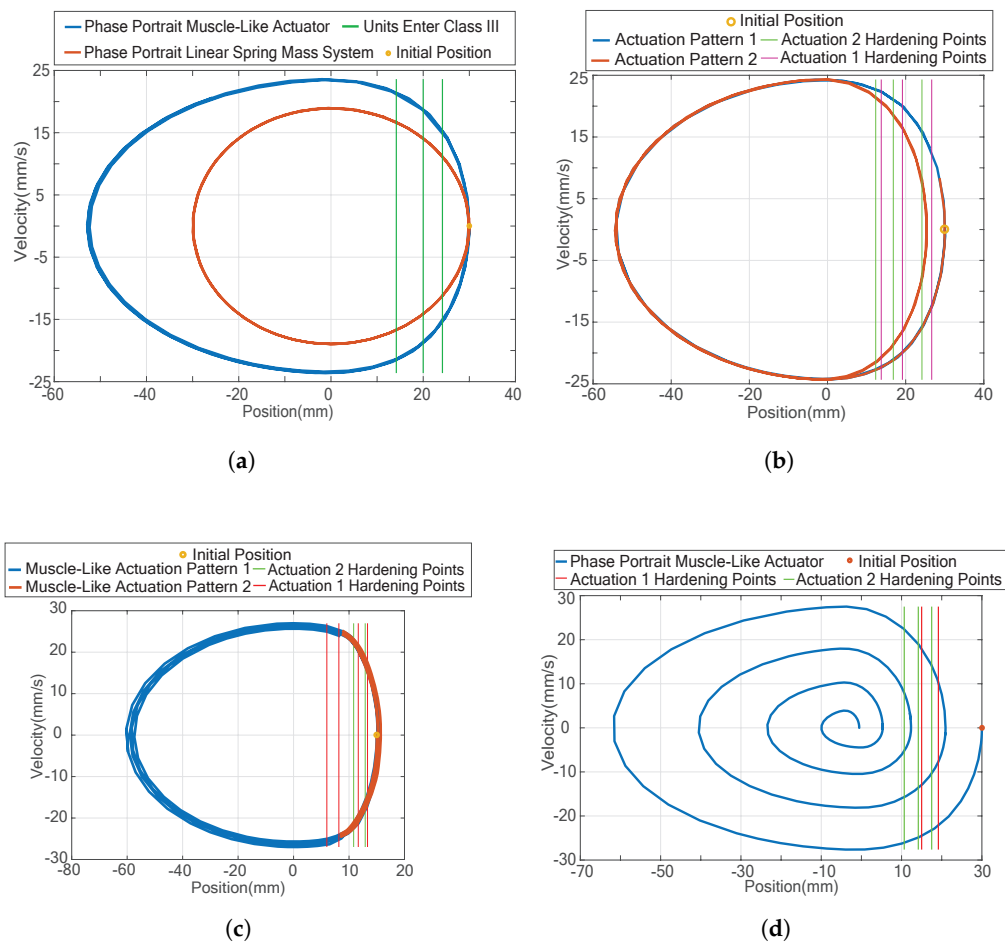


**Figure 8.** Actuator phase portraits of different switching patterns: (a) simple-harmonic motion of variable stiffness actuator; (b) switching based upon time; (c) switching based upon position; and (d) switching activation based upon velocity.

### 3.3. SEA Model Implementation

The motivation behind the development of the SEA model is to use standard state space control methods in designing an linear observer to reconstruct the state for full state feedback control. The observer captures the nominal linear behavior of the average stiffness; it does not account for the nonlinearities in the plant due to the hardening behavior. The crucial aspect of using this model, however, is how control of a discretized plant with all of its complexity is accomplished using a simple linear observer architecture based only on measurement of the load position.

The Series Elastic Actuator was originally developed by Pratt and Williamson (see [4] for simple model development and control designed for use with their actuator). The model used in the work for this project borrows concepts from Pratt and other developments in the SEA [10,11]. For this project, a model was developed using a linear motor, a spring and a load mass. This greatly simplifies a model in which each motor unit is treated as its own mass-spring-damper system coupled together in series-parallel configurations. Such a model would reach extremely high order state spaces with even one or two actuation units coupled together. The SEA model sufficiently captures all the dominant dynamic effects of the actuator system.

Following the procedure for designing an observer as presented in Brogan [12] and Sinha [13], the necessary steps were taken to create an observer using the SEA model discussed previously, see Figure 9a,b.

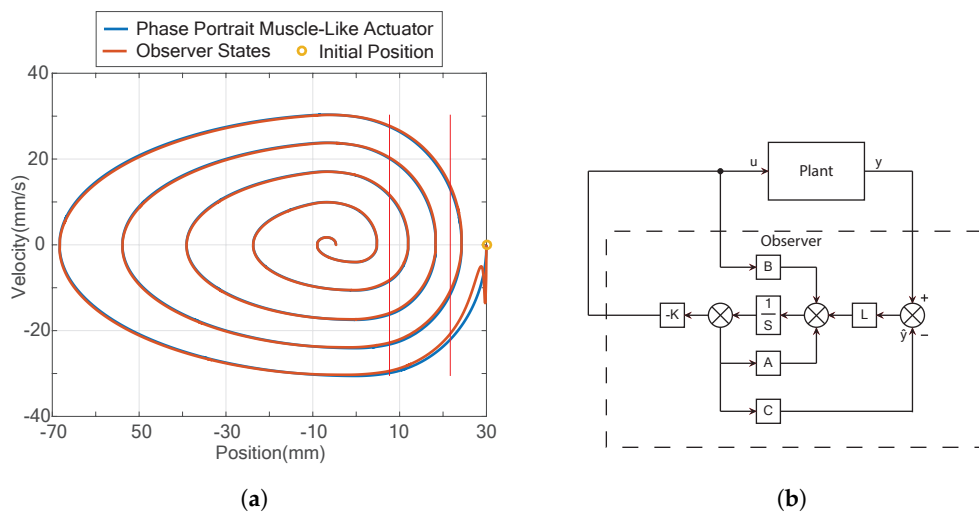


**Figure 9.** Observer feedback loop and phase portrait: (a) phase portrait with observer; and (b) observer with full state feedback control.

For any linear system, this would give the controller for the system, however, the discrete muscle-like actuator has one last important characteristic which has not yet been discussed thoroughly. The muscle-like discrete actuator must receive a quantization of the control input  $u$  in order to actuate the particular motor units needed to generate the force dictated by the controller. The output,  $u$ , of the controller is a continuously real-valued variable which must be translated to a discrete number of motor units “on”, an integer value [14]. This section examines this problem and shows the novel solution implemented and the initial value simulations that resulted from this solution.

### 3.3.1. Quantization of the Observer Control Signal to Discrete Control Signal

The produced force of the actuator at any given length can be obtained using Equation (4) after using the matrix Equations (9)–(12) to solve for the individual actuation unit lengths. Two similar methods of quantizing the control input from the controller are explained. Method I is by constant scaling of the force, length and approximating the number of total motor units active; this method computes the force available for the current actuator length that is closest to the control input,  $u$ . Method II is a lookup table that is generated off-line and referenced during run-time; this method searches for the force in the table that is closest to the control input and selects the activation pattern associated with the force. We must perform these steps separately from the control because the individual actuation unit lengths,  $l_i$ , are unknown. Figure 10a shows the muscle-like actuator given an initial position and zero initial velocity and displays how the controller is able to converge on the equilibrium point. It must be noted that given the nature of quantized control the system will not converge exactly to the equilibrium point but will instead converge within a certain radius  $R$  of a sphere inscribed within an ellipsoid [15]. Using the second method of pre-computing, a lookup table that is referenced in run-time gives the results seen in Figure 10b.

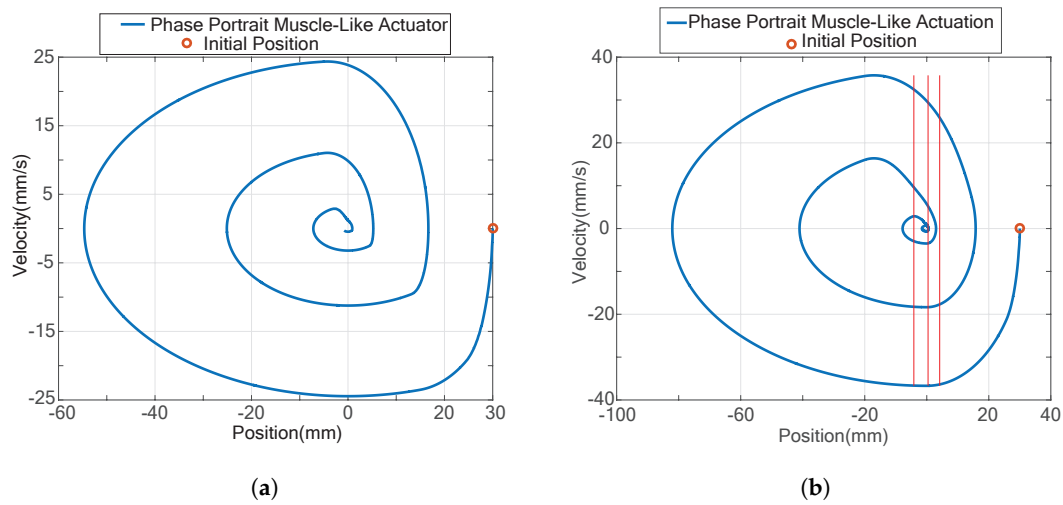


**Figure 10.** Observer control phase portraits with two different discrete quantization methods: (a) quantization Method I; and (b) quantization Method II.

### 3.3.2. Introducing a Disturbance

To observe how the actuator behaves when disturbances perturb the system, a constant disturbance force is introduced. This was analyzed for the open loop velocity switching condition and for both of the two methods discussed above for the quantization of the control signal. The results can be seen in Figures 11 and 12b. Notice in the two figures with the Observer control methods that both of them only converge to a certain point but then enter a cycle of constant oscillations. This region of the phase portrait shows that the actuator does not receive valid control input for this region. The reason for this is that when the actuator is in Class Zero, it does not matter what pattern or activation level is switched to; in this mode of the actuator, it can impose no force and therefore is not controllable.

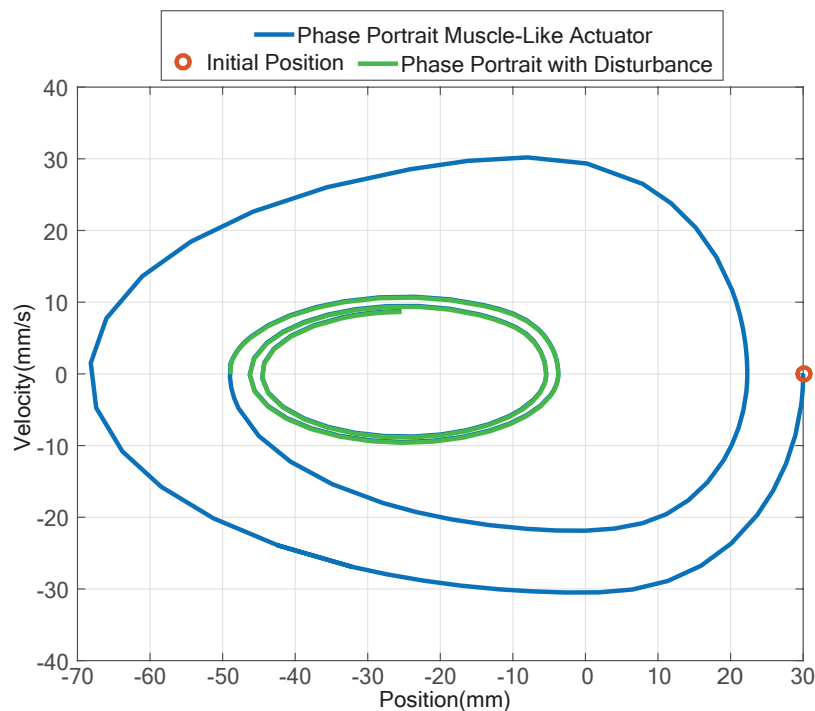


**Figure 11.** Velocity switching with disturbance force.

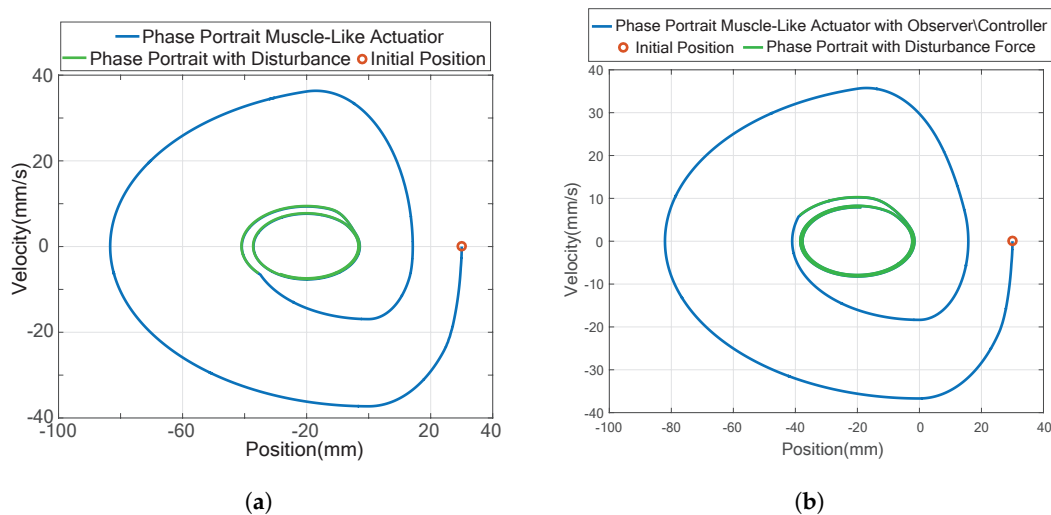


**Figure 12.** Introduction of a disturbance force into the system: (a) control Method I with disturbance (green); and (b) control Method II with disturbance (green).

### 3.3.3. Muscle-Like Actuator in Antagonistic Setup

In order not to lose controllability in certain regions of the statespace, an antagonist actuator setup using two variable stiffness discrete muscle-like actuators can be utilized (see Figure 13). In this scenario, the SEA model used as the observer maintains a strong performance and gives a good estimation of the states of the antagonistic actuator setup. Here it must be explained why the observer model was not reconfigured for an antagonistic SEA model and how the antagonistic muscle-like actuator is superior to the antagonistic SEA. The answer is really quite simple, as stated in [16] and also proven through analysis of the controllability matrix. An antagonistic SEA model with linear springs of the same spring constant is not controllable because the stiffness of the SEA model becomes independent of the controllable parameters. Figure 14 shows such a setup. Summing the forces acting on the mass in the center gives Equation (13). The stiffness of this setup is given by Equation (14) [16] and shows that the result for the stiffness is dependent only on the constant  $k$  which is not variable and therefore renders this setup uncontrollable. Thus, considering that argument forward progress can be made with the same observer used in the previous section and shown in Figure 15a, the result of using an antagonist actuator in place of the return spring. This result is easily seen to be much improved from the results of the actuator with a return spring, which should make sense because in an antagonistic setup there is no longer a Class Zero region where the actuator is uncontrollable.

$$\begin{aligned}
 F &= -k(x - x_{0A}) + k(x_{0B} - x) \\
 &= -2k + k(x_{0A} - x_{0B})
 \end{aligned}
 \tag{13}$$

$$K = \frac{dF}{dx} = -2k
 \tag{14}$$

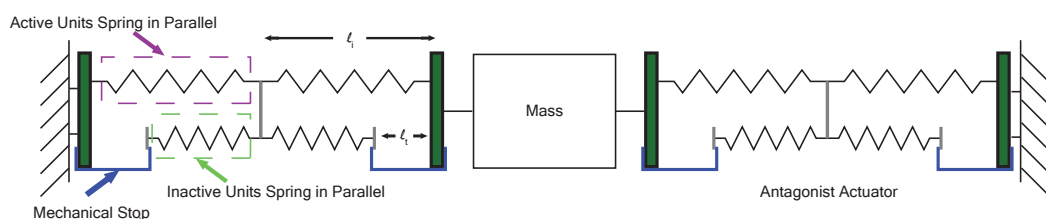


**Figure 13.** Antagonistic actuator setup.

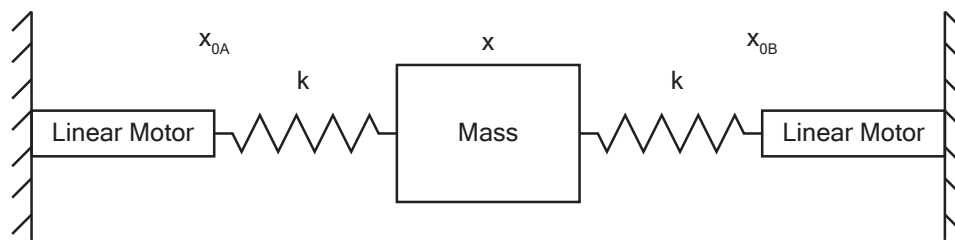


Figure 14. Demonstration of the uncontrollable linear springs.

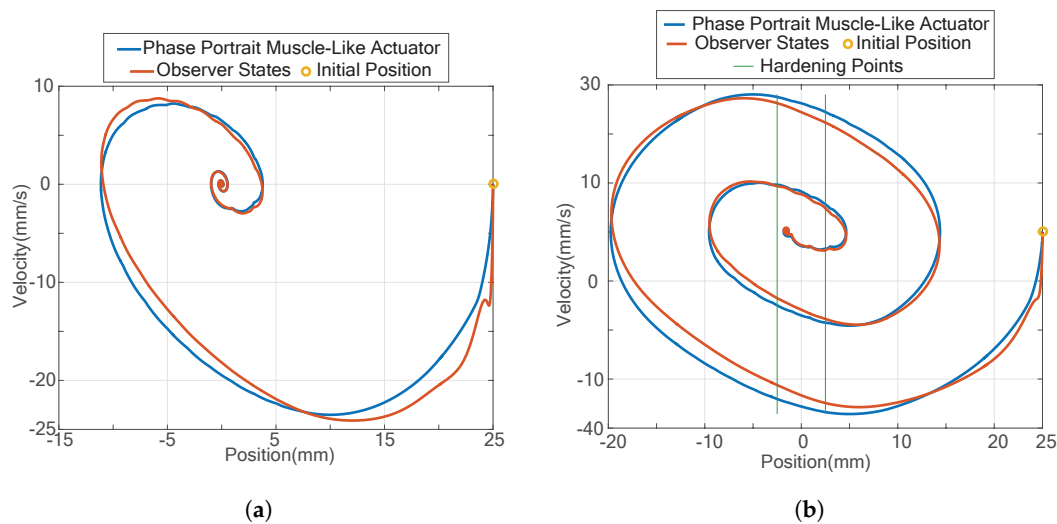


Figure 15. Antagonist control phase portraits: (a) antagonistic control with observer; and (b) antagonistic control with observer and disturbance Force.

#### 4. Experimental Verification of Length-Based Hardening

To verify the variable stiffness characteristics discussed in Sections 2.1–2.3, an experiment was designed that would enable the actuator to be given an actuation pattern and then steadily lengthened while keeping the activation pattern constant throughout. The setup of the experiment can be seen in Figure 16 and is described as follows. A chain of four actuation units of the type described in Mathijssen et al. [2] (see Figure 16) makes up an actuator mounted between two fixtures where one of the fixtures is secured to an optical table while the other fixture is mounted to a micrometer stage. In series with the actuator is a Futek 1lb force cell whose voltage output was measured using a LeCroy (WaveRunner 604Zi, Teledyne LeCroy, Rockland County, NY, United States) oscilloscope. The fixture mounted on the micrometer stage gave the ability to lengthen the actuator in steps as fine as 0.025 mm, however, for this experiment steps of approximately 1.2 mm were sufficient. The drive circuitry supplying current to each motor unit is a custom design, described in Mathijssen et al. [2]. The digital signal supplied to the circuitry is from an National Instruments DAQ and manually activated through a National Instruments LabView Virtual Instrument. Taking data sets was performed by setting a constant activation pattern and then increasing the length of the actuator in steps of approximately 1.2 mm, the actual excursion recorded directly from the micrometer stage, and measuring the force at each step. This was repeated with a different activation pattern after resetting the stage. At the extremes of extension, the restoring force of the spring overcame the magnetic force holding the solenoid plunger in the solenoid housing, and data points could not be collected beyond this ultimate length, which varied with the activation pattern (in practice, this ultimate length constitutes failure and should be avoided). Table 2 shows the activation patterns that were used in the experiment and

their corresponding activation levels and the figure where their data is graphed and compared to the theoretical model.

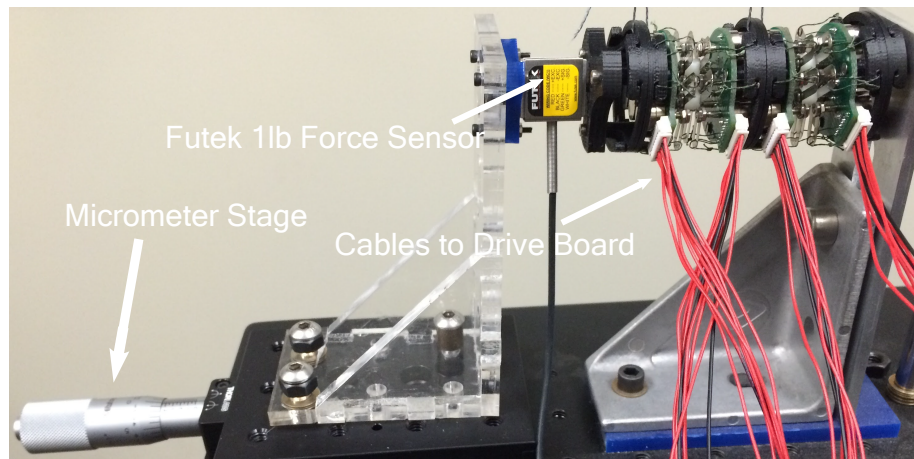
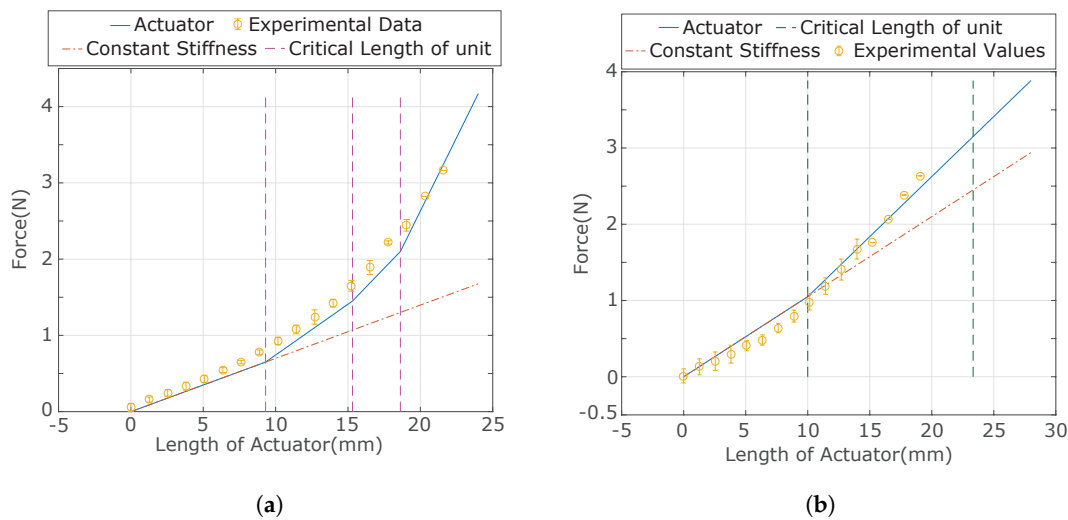


Figure 16. Experimental hardware setup.

Table 2. Experimental actuation patterns.

Pattern	Activation Level	Figure
[4 0 1 3]	8	Figure 17a
[6 2 0 0]	8	Figure 17b

The experiment was performed for different actuation patterns and levels. The experiment was also run for the same actuation level repeatedly, while varying which motor unit was used; to evaluate the effects of manufacturing variations, the motor units were activated in different combinations. For example, if the activation level is 4 for a certain actuation cell, then given a total number of motor units of six, the different combinations for activation four motor units is given  $\binom{n}{k} = \frac{n!}{k!(n-k)!}$  for a total of 15. Figure 17a shows the experimental data plotted with standard deviation error bars with an activation pattern of [4 0 1 3]. This plot includes four data sets for the same activation pattern just with different choices for which solenoid to activate from those available on each cell. Although there is some deviation in the slope of each segment due to manufacturing variation, the hardening trend described in Section 2 is evident. The data stop before the actuator reaches the last hardening point of the actuator, this happens because the restoring force of the springs became too great and overcame the magnetic field of one or more of the motor units. The plot shown in Figure 17b shows a different activation pattern but the same activation level, eight motor units. Note that this activation pattern has different hardening behavior than the previous one and the data follows the trend predicted by the model. Again, the data do not go to excursions as far as the model predicts because the spring force overcame the magnetic field force. This is a limitation of Mathijssen and coworkers’ platform (or the line electric solenoid/drive board), not the theory in and of itself.



**Figure 17.** Length dependent hardening: (a) experimental hardening vs. theoretical hardening—Pattern: 4013; and (b) experimental hardening vs. theoretical hardening—Pattern: 6200.

## 5. Conclusions and Future Work

The work presented in this article characterizes the length dependent hardening behaviors encountered in the use of discrete muscle-like actuators. This characterization is done through the introduction of a Class system that defines the regions for which an actuation unit will experience different stiffness values. It is noted that different stiffness values for the actuator can be achieved while keeping the activation level constant, through a simple change in the activation pattern. This behavior of length dependent hardening is validated through the experiment shown in Section 4.

A control method that simplifies the complex nature of discrete actuator control, by exploiting the similar qualities of an SEA and implementing a linear observer to reconstruct the state and deploy a full-state feedback control law is also presented in this article. The challenges associated with applying a continuously varied control signal to a discrete number of motor units “on” necessitates the development of a quantization method that approximates the best activation level and pattern for the control signal.

Future work for this concept includes conducting dynamic experiments with a moving mass while using the observer architecture as the hardware improves with better design and manufacturing processes for discrete actuators incorporating the three main properties: compliance, modularity, and redundancy. We also desire to research a more general framework and control strategy for more complex hierarchical arrangements of discrete actuators.

**Acknowledgments:** This work was partially supported by NSF CNIC: US-Belgium Engineering Planning Visit: Simplified Models for Bio-inspired Actuators Grant 1427787. The authors would like to express their thanks to Glenn Mathijssen and Dr. Bram Vanderborght in Brussels, Belgium for the helpful conversations that spurred on the work shown in this paper.

**Author Contributions:** Caleb Fuller and Joshua Schultz conceived and designed the experiment; Caleb Fuller performed the experiment and analyzed the data; Caleb Fuller wrote the paper; Joshua Schultz provided edits and ideas for writing the paper.

**Conflicts of Interest:** The authors declare no conflicts of interest.

## References

1. Enoka, C. Motor Unit. *Compr. Physiol.* **2012**, *2*, 2629–2682.
2. Mathijssen, G.; Schultz, J.; Vanderborght, B.; Bicchi, A. A muscle-like recruitment actuator with modular redundant actuation units for soft robotics. *Robot. Auton. Syst.* **2015**, *74*, 40–50.
3. Gere, J.; Goodno, B. *Mechanics of Materials*; Cengage Learning: Boston, MA, USA, 2008.

4. Pratt, G.A.; Williamson, M.M. Series elastic actuators. In Proceedings of the 1995 IEEE/RSJ International Conference on Intelligent Robots and Systems 95. "Human Robot Interaction and Cooperative Robots", Pittsburgh, PA, USA, 5–9 August 1995; Volume 1, pp. 399–406.
5. Vanderborght, B.; Albu-Schaeffer, A.; Bicchi, A.; Burdet, E.; Caldwell, D.G.; Carloni, R.; Catalano, M.; Eiberger, O.; Friedl, W.; Ganesh, G.; et al. Variable impedance actuators: A review. *Robot. Auton. Syst.* **2013**, *61*, 1601–1614.
6. Tonietti, G.; Schiavi, R.; Bicchi, A. Design and Control of a Variable Stiffness Actuator for Safe and Fast Physical Human/Robot Interaction. In Proceedings of the 2005 IEEE International Conference on Robotics and Automation, Barcelona, Spain, 18–22 April 2005.
7. Schultz, J.; Mathijssen, G.; Vanderborght, B.; Bicchi, A. A selective recruitment strategy for exploiting muscle-like actuator impedance properties. In Proceedings of the 2015 IEEE/RSJ Intelligent Robots and Systems Conference, Hamburg, Germany, 28 September–2 October 2015; pp. 40–50.
8. Corr, L.R.; Clark, W.W. Comparison of low-frequency piezoelectric switching shunt techniques for structural damping. *Smart Mater. Struct.* **2002**, *11*, 307, doi:10.1088/0964-1726/11/3/307.
9. Gasparri, G.M.; Garabini, M.; Pallottino, L.; Malagia, L.; Catalano, M.; Grioli, G.; Bicchi, A. Variable Stiffness Control for Oscillation Damping. In Proceedings of the 2015 IEEE/RSJ Intelligent Robots and Systems Conference, Hamburg, Germany, 28 September–2 October 2015; pp. 6543–6550.
10. Rahman, S.M.M. A novel variable impedance compact compliant series elastic actuator for human-friendly soft robotics applications. In Proceedings of the IEEE International Workshop on Robot and Human Interactive Communication, Paris, France, 9–13 September 2012; pp. 19–24.
11. Braun, D.J.; Petit, F.; Huber, F.; Haddadin, S.; Van Der Smagt, P.; Albu-Schaeffer, A.; Vijayakumar, S. Robots driven by compliant actuators: Optimal control under actuation constraints. *IEEE Trans. Robot.* **2013**, *29*, 1085–1101.
12. Brogan, W. *Modern Control Theory*, 3rd ed.; Prentice Hall: Upper Saddle River, NJ, USA, 1991; pp. 532–533.
13. Sinha, A. *Linear Systems: Optimal and Robust Control*; CRC Press: Boca Raton, FL, USA, 2007.
14. Schultz, J.A.; Ueda, J. Intersample discretization of control inputs for flexible systems with quantized cellular actuation. In Proceedings of the ASME 2010 Dynamic Systems and Control Conference, Cambridge, MA, USA, 12–15 September 2010; American Society of Mechanical Engineers: New York, NY, USA, 2010; pp. 421–428.
15. Corradini, M.L.; Orlando, G. Robust quantized feedback stabilization of linear systems. *Automatica* **2008**, *44*, 2458–2462.
16. Van Ham, R.; Thomas, S.; Vanderborght, B.; Hollander, K.; Lefeber, D. Review of Actuators with Passive Adjustable Compliance/Controllable Stiffness for Robotic Applications. *IEEE Robot. Autom. Mag.* **2009**, doi:10.1109/MRA.2009.933629.

